Available online at www.sciencedirect.com
SCIENCE DIRECT®
Applied Catalysis A: General 309 (2006) 62–69
APPLIED CATALYSIS A: GENERAL
www.elsevier.com/locate/apcata

Studies on the structural change of a reaction-controlled phase-transfer $[\pi\text{-}C_5H_5NC_{16}H_{33}]_3\{PO_4[WO_3]_4\}$ catalyst during the selective oxidation of cyclopentene to glutaric acid with aqueous H_2O_2

Hui Chen [a], Wei-Lin Dai [a,*], Xin-Li Yang [a], Ruihua Gao [a,b], Yong Cao [a], Hexing Li [b], Kangnian Fan [a]

[a] *Department of Chemistry and Shanghai Key Laboratory of Molecular Catalysis and Innovative Materials, Fudan University, Shanghai 200433, PR China*

[b] *Department of Chemistry, Shanghai Normal University, Shanghai 200234, PR China*

Received 16 February 2006; received in revised form 17 April 2006; accepted 24 April 2006
Available online 30 May 2006

Abstract

The selective oxidation of cyclopentene to glutaric acid (GAC) with aqueous hydrogen peroxide was carried out over a reaction-controlled phase-transfer catalyst—$[\pi\text{-}C_5H_5NC_{16}H_{33}]_3\{PO_4[WO_3]_4\}$. The high GAC yield of 83.1% was obtained on the fresh catalyst, while a much higher GAC yield of 98.8% was obtained over the recovered catalyst. The fresh catalyst, the one under reaction conditions and the recovered ones were all characterized by TG, FT-IR, Raman and ^{31}P NMR spectroscopy. It is interesting to find that the atomic content of tungsten and phosphorous as well as the molecular structure of the fresh catalyst all change after the reaction. ^{31}P NMR results reveal that under the treatment with high concentration hydrogen peroxide the insoluble catalyst can degrade into smaller and active species, which is soluble in the reaction mixture and can transfer oxygen to the C=C bond, resulting in the selective cleavage of cyclopentene to glutaric acid. After the complete consumption of hydrogen peroxide, the smaller and active tungsten species will polymerize into $(PW_{11}O_{39})^{7-}$ and $(PW_{12}O_{40})^{3-}$ with stable Keggin structure by forming W–O_c–W (edge-sharing) bond. These compounds are insoluble and will precipitate from the reaction mixture after the reaction when hydrogen peroxide is used up, making it much convenient for recovering and reusing.
© 2006 Elsevier B.V. All rights reserved.

Keywords: Cyclopentene; Glutaric acid; Selective oxidation; Hydrogen peroxide; Reaction-controlled phase-transfer catalyst

1. Introduction

Dicarboxylic acids, including glutaric acid, adipic acid, trimethyladipic acid and dodecanedioic acid, are essential feedstocks for the manufacture of polyamides, polyesters, plasticizers and lubricating oils [1]. The anhydrides, one of the monomer of LCD materials, are also synthesized from dicarboxylic acids. However, there is no convenient method for the production of glutaric acid yet, especially in large-scale industry. The current manufacture is in a multi-step process by oxidative cleavage of C–C bond of mixtures containing the corresponding cyclic alcohols and ketones and their derivatives with nitric acid [2–4]. Noyori et al. [5,6] has developed a general method of synthesizing carboxylic acids, including adipic acid and glutaric acid, in which Na_2WO_4 and $[CH_3(n\text{-}C_8H_{17})_3N]HSO_4$ were used as the oxidation and phase-transfer catalysts, respectively, and the latter is much expensive and cannot be easily separated and recovered. Thus, this process is impossible for large-scale industrial production of glutaric acid.

In our group, a novel green process of synthesizing glutaric acid from cyclopentene with high GAC yield of 92.3% has been developed without using any kinds of solvents, in which only 50% aqueous H_2O_2 solution and tungstic acid were used as the oxidant and the catalyst, respectively [7]. However, although no organic pollution arises during the whole process, tungstic acid can dissolve in the aqueous solution of H_2O_2 and form a homogeneous catalyst—$H_2[W_2O_3(O_2)_4(H_2O)_2]$, which is difficult to be recovered and reused after the reaction. In addition, the high content of tungsten contaminant in the final product makes this process much inconvenient for its further purification.

* Corresponding author. Tel.: +86 21 55664678; fax: +86 21 65642978.
E-mail address: wldai@fudan.edu.cn (W.-L. Dai).

0926-860X/$ – see front matter © 2006 Elsevier B.V. All rights reserved.
doi:10.1016/j.apcata.2006.04.037

Therefore, the problem diverts to the finding of new catalyst that is easy to be recovered and reused. The polyoxometalates (POMs) catalyst system was studied intensively by Venturello [8–12] and Ishii [13–19], among which the quaternary ammonium heteropolyoxotungtates were synthesized and used in the epoxidation of olefins with high activity and selectivity. These catalysts, with the active cation $\{PO_4[W(O_2)_2]_4\}^{3-}$, are named as Ishii-Venturello catalysts, and attracts much interest in many fields [20–27], including the selective oxidation of 1,2-diols to carboxyl acids [9]. Recently, Xi et al. [28] reported a reaction-controlled phase-transfer catalyst—$[\pi\text{-}C_5H_5NC_{16}H_{33}]_3\{PO_4[WO_3]_4\}$, which is active and selective for the epoxidation of propylene with 30% H_2O_2. More interestingly, this catalyst is insoluble in both water and organic solvent, but can dissolve in organic solvent after the treatment with H_2O_2 and can catalyze the reaction homogeneously. After the reaction, it precipitates itself from the reaction mixture and can be easy to be recovered.

However, the unique character of this reaction-controlled phase-transfer catalyst has not been tried in other reactions yet. Considering the similarity of the reaction system from Zuwei with ours, this catalyst may show good catalytic performance as well as easy recovering ability in the selective oxidation of cyclopentene to glutaric acid. In addition, although the nature of this catalyst and the structure change involved in the epoxidation has been investigated [29,30], the intrinsic structure change was not clearly established yet. In this paper, the excellent catalytic performance and the unique reaction-controlled character of this catalyst were reported. The fresh catalyst, the one under reaction conditions and the recovered ones were all characterized by TG, FT-IR, Raman and ^{31}P NMR spectroscopy.

2. Experimental

2.1. Preparation of $[\pi\text{-}C_5H_5NC_{16}H_{33}]_3\{PO_4[WO_3]_4\}$ and $[\pi\text{-}C_5H_5NC_{16}H_{33}]_3\ [PW_{12}O_{40}]$

The catalyst $[\pi\text{-}C_5H_5NC_{16}H_{33}]_3\{PO_4[WO_3]_4\}$ was prepared according to the procedure described previously [30,31]. A suspension of tungstic acid 2.5 g (10 mmol) in 7 mL of aqueous H_2O_2 (35%) was stirred and heated to 60 °C until a colorless solution was obtained. The solution was filtered and then cooled to room temperature. After that, 40% (w/v) H_3PO_4 (0.62 mL, 2.5 mmol) was added to the solution, which was then diluted to 30 mL with distilled water. An amount equal to 1.80 g of cetylpyridiniumammonium chloride (5 mmol) in dichloromethane (40 mL) was added dropwisely with stirring in 2 min, and the mixture was maintained for an additional 15 min. The organic phase was then separated, dried with anhydrous Na_2SO_4, filtered and evaporated under atmospheric pressure at 50–60 °C (water bath). At last, about 2.5 g (85%, based on the quaternary ammonium salt charged) of the dried yellow powder was obtained by further evacuation, labeled as A1.

The catalyst $[\pi\text{-}C_5H_5NC_{16}H_{33}]_3[PW_{12}O_{40}]$ was prepared as follows. Solution A is prepared by dissolving 5 g $H_3PW_{12}O_{40}$ in distilled water, and solution B is prepared by dissolving 1.87 g $\pi\text{-}C_5H_5NC_{16}H_{33}Cl$ in distilled water. Then solution B was added dropwisely into solution A with stirring. After the white precipitation was formed, the suspension was stirred for an additional 4 h, and then filtered and washed with distilled water. White powder was obtained after further drying, labeled as A2. The recovered catalysts of A1 and A2 are labeled as Re-A1 and Re-A2, respectively.

2.2. Catalytic oxidation of cyclopentene to glutaric acid

A round-bottomed flask with a condensation tube was charged with the catalyst (0. 165 g), 50% H_2O_2 (6 mL) and cyclopentene (Fluka, 2 mL). The flask was then placed in a water bath at 48 °C with vigorous stirring until the reflux of cyclopentene ended. Then the temperature was rosen to 85 °C and hold for another 8 h. After then, the resulting suspension was centrifugated and the pellucid liquid was analyzed by titration with NaOH solution to get the yield of organic acid. The precipitated catalyst was recovered for further use.

The pellucid liquid was boiled to bubbling up to decompose the excess H_2O_2 (avoid explosion while vacuum distillation), until the amylum-KI test is negative. Then small amounts of activated carbon were added and the mixture was stirred in boiling water bath for 30 min. After filtered, the colorless solution was vacuum distilled and concentrated to remove most of the water. After that, the resulting solution was refrigerated at 0 °C for 24 h and colorless GAC crystal was formed. After filtered and washed with small amounts of ice water, the as-obtained crystals were dried at 90 °C for 12 h for the future analysis. The filtrate can be further dehydrated to get more GAC crystals that can be mixed with those from the first time for the accurate analysis of pure GAC yield. The yield of glutaric acid was determined with acid-base titration, while the purity of glutaric acid was analyzed with melting point test, HPLC and GC (after esterification with methanol).

2.3. Catalyst characterization

Thermogravimetry differential thermal analysis (TG/DTA) was performed by using Perkin-Elmer TGA7/DTA7 thermal analysis system under air atmosphere (50 mL min^{-1}) with a heating rate of 10 K min^{-1}. The laser Raman experiments were performed by using a Jobin Yvon Dilor Labram I Raman spectrometer equipped with a holographic notch filter, a CCD detector and He-Ne laser radiating at 632.8 nm. The FT-IR measurements were carried out with a Nicolet Model 205 spectrometer, using KBr pellet technique. ^{31}P NMR spectra of reaction solution and solid catalysts were collected in a Brucker DXR 400 spectrometer.

3. Results and discussion

3.1. Selective oxidation of cyclopentene to glutaric acid

The oxidation of cyclopentene to glutaric acid was carried out with the reaction-controlled phase-transfer catalyst A1 and

Table 1
Selective oxidation of cyclopentene to glutaric acid on the catalyst A1, A2 and tungstic acid

Catalyst	30% H_2O_2 as the oxidant		50% H_2O_2 as the oxidant	
	Yield of GAC (%)	TOF (min^{-1})	Yield of GAC (%)	TOF (min^{-1})
A1	79.5	4.4	83.1	13.3
A2	77.2	0.24	85.6	0.38
H_2WO_4	80.1	0.26	92.3	0.67

Reaction conditions: cyclopentene (2 mL); catalyst (W): H_2O_2: cyclopentene = 0.015:4.4:1 (molar ratio); at 85 °C for 8 h. The yield of GAC was based on cyclopentene.

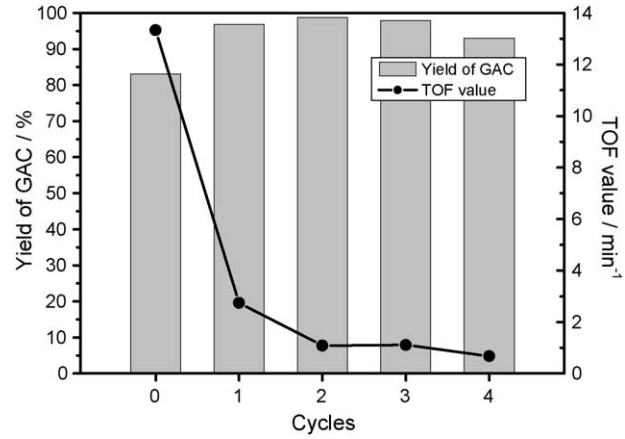

Fig. 1. The recovering and reusing conditions of catalyst A1. Reaction conditions: cyclopentene (2 mL); for fresh catalyst, catalyst (W):H_2O_2:cyclopentene = 0.015:4.4:1 (molar ratio). After reaction the catalyst is recovered by centrifugation, washed with water and dried. Then it was used again in the second run by the addition of same quantity of H_2O_2 and cyclopentene. All reactions were carried out at 85 °C for 8 h. The yield of GAC was based on cyclopentene.

50% hydrogen peroxide, without using any solvents and any other additives. The reaction is so vigorous that the disappearance of cyclopentene can be observed within 5 min, compared with that of 120 min in the reaction catalyzed by homogeneous tungstic acid. During the reaction, the solid catalyst dissolved firstly, and two phases changed into one phase, and then a pellucid solution was obtained. After the reaction being performed at 85 °C for 3–5 h, the catalyst precipitated itself from the reaction system. Therefore, the catalyst can be recovered easily by simply filtration or centrifugation after the reaction. The catalyst A2 was also used in this reaction for the purpose of comparison, which can also be dissolved in the reaction mixture during the reaction and precipitate when H_2O_2 is consumed up, thus it also exhibits the characteristic of reaction-controlled phase-transfer catalysis. However, much more time is needed for A2 to be dissolved. The catalytic performance and TOF values of A1, A2 are shown in Table 1.

As can be easily seen from Table 1, the GAC yield over A1 is 83.1% with 50% H_2O_2, a bit lower than the homogeneous catalyst. But the TOF value of A1 is 35 times higher than that of homogeneous tungstic acid. The phase-transfer catalyst A1 shows much higher activity than the other ones. In addition, the yield of GAC on catalyst A2 (85.6%) is similar as on A1, even a bit higher than that of A1, but the TOF value (0.38 min^{-1}) is much lower than that of A1 (13.3 min^{-1}). The same tendency was also obtained with 30% H_2O_2 as the oxidant. In conclude, the activity of catalyst A1 is the highest among the three catalysts, though the yield of GAC is not in that case. As discussed in our previous work, this reaction is an acid-catalyzed one [7], thus the acidic condition of the reaction media may play an important role in the oxidative cleavage of cyclopentene with H_2O_2. It is well known that a solution with high acidity was obtained (pH −0.23) after the tungstic acid was dissolved in 50% H_2O_2. When cyclopentene was added, the reaction started, and the pH value increased. After the disappearance of cyclopentene, the pH value is 0.25. However, in the systems with A1 and A2 as the catalysts, the pH values are much lower than that with tungstic acid, which are 0.53 and 0.50, respectively. Hence, the difference of acidity may be one of the reasons why the yield of GAC on catalysts A1 and A2 is not as high as that on tungstic acid. In order to know if the yield of GAC can be increased with the increase of acidity, H_2SO_4 ($n_{H_2SO_4} : n_W = 1 : 1$) was added to the A1 and A2 reaction systems. However, opposite results are obtained. The yields decreased a bit for either A1 or A2, suggesting that the dissociative H^+ by the addition of H_2SO_4 cannot contribute to the oxidative cleavage of cyclopentene with H_2O_2. Only the H^+ produced by the action of H_2O_2 with tungsten-species can improve the catalytic performance.

The recovering and reusing behavior of catalyst A1 is also investigated, as shown in Fig. 1. Much interestingly, the yield of GAC on the recovered catalyst reaches 98.8%, much higher than that of the fresh catalyst, even 5% higher than that of the homogeneous tungstic acid catalyst. It is also very surprising to find that the yield of GAC was still very high and maintained at a value above 93.0% even it was reused for four times. However, the TOF values dropped abruptly from 13.3 min^{-1} of the fresh one to 2.7 min^{-1} of the recovered one (one cycle), and decreased along with the recover times, suggesting that the reaction rate was decreased toward the recovered catalyst, and the active sites of the recovered catalyst was different with that of the fresh one. In addition, it was observed that the TOF value of the recovered catalysts changed with the recycle times, although it changed little with the second and the third cycle. However, the recovery efficiency is not very high, only about 70 wt.%(±10%) of the working catalyst can be recovered even toward those with the TOF value unchanged. Thus, the intrinsic nature of the active site changed definitely during the recovering process, even one cycle by another. For all these catalysts, the purity of the resulting glutaric acid solid is better than 99% (analyzed by GC) and the melting point is 96–97 °C, similar to the literature value of 97–98 °C. So the resulting GAC product synthesizing in this process is pure enough to be used directly in most fields without any further purification.

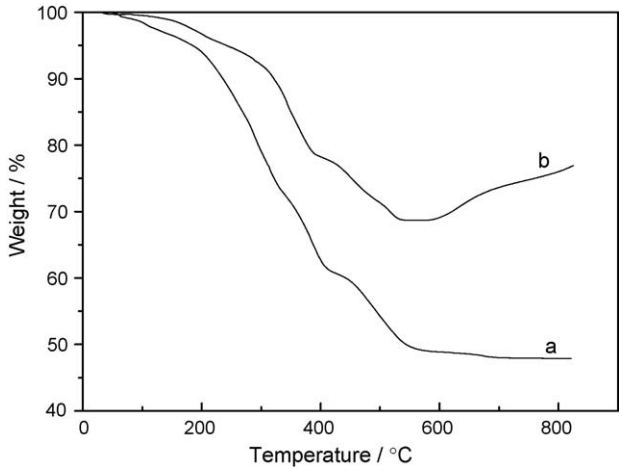

Fig. 2. TG figures of catalyst (a) A1 and (b) Re-A1.

3.2. TG

The TG profiles of catalyst A1 and Re-A1 are shown in Fig. 2. The catalyst decomposes and the weight losses appear when it is heated at elevated temperature. The quaternary ammonium cation is lost firstly, and phosphate anion will be lost secondly. At last, when the temperature is higher than 700 °C, only WO_3 is left in the residue. The maximum weight loss ratio is 52.1%, same as the theoretical value. For the recovered catalyst, the TG profile is quite different from the fresh one. The weight loss ratio decreases at temperature lower than 545 °C because of the loss of quaternary ammonium cation and phosphate anion, respectively. However, the weight loss percent increases if the temperature is risen above 600 °C, which is very surprising because the TG experiment is carried out in air atmosphere, no other elements but oxygen can be combined to the residue of the recovered catalyst after treated at high temperature. Considering the color of the recovered catalyst is light purple, different from that of the fresh yellow one, one can think that maybe some W species were reduced to lower oxidation states than +6 during the recovering process, for instance, tungsten blue was formed after the reaction. Therefore, the weight of the catalyst rises when the W species with lower states was oxidized to WO_3. The final weight loss ratio is 23.3% to the recovered catalyst, much lower than that of the fresh one, implying that the W content in the recovered catalyst is much higher than that of the fresh one, and the structure of the recovered catalyst is different from the fresh one.

From the TG result, it is very easy to find that the WO_3% (weight percent) in the recovered catalyst Re-A1 is 76.7%, while in the catalyst A2 it is 73.4% (calculated according to the molecular formula: $[\pi\text{-}C_5H_5NC_{16}H_{33}]_3[PW_{12}O_{40}]$). These two values are very close to each other, but very different in contrast to 47.9% of the fresh one A1, which suggests the possibility that the recovered catalyst Re-A1 has similar molecular structure as that of A2.

3.3. Raman spectra

In order to provide better understanding of the structural changes of the A1 catalyst after the reaction, the fresh catalyst A1, A2 and the recovered one Re-A1, Re-A2 were all characterized by Raman spectroscopy. In order to give a better assignment of the Raman bands of the catalysts, phosphatotungstic acid was also measured by Raman spectroscopy under the same conditions, as shown in Fig. 3.

In the 100–1500 cm^{-1} range of Raman spectra, no Raman band at 1031 cm^{-1} is observed for the phosphatotungstic acid sample (Fig. 3(e)), which is a clear indication for the absence of the quaternary ammonium cation. According to the reference, the band at 648 cm^{-1} is also attributed to the quaternary ammonium cation [30]. From Fig. 3(A(a)), A1 shows Raman bands at 314, 552, 648, 887, 964 and 1031 cm^{-1}. Those peaked at 314, 552 and 964 cm^{-1} can easily be assigned to $\upsilon(W\text{–}O_2H)$, $\upsilon[W(O_2)]$, $\upsilon(W{=}O)$, respectively [20,32], indicating that there is active oxygen in the structure of the fresh catalyst A1, which may be one of the reasons for the ultra high activity of the reaction-controlled phase-transfer catalyst. The weak band at 887 cm^{-1} is due to the presence of excess free hydrogen peroxide [20], which maybe entrapped during the preparation process. As mentioned above, the bands at 648 and 1031cm^{-1}

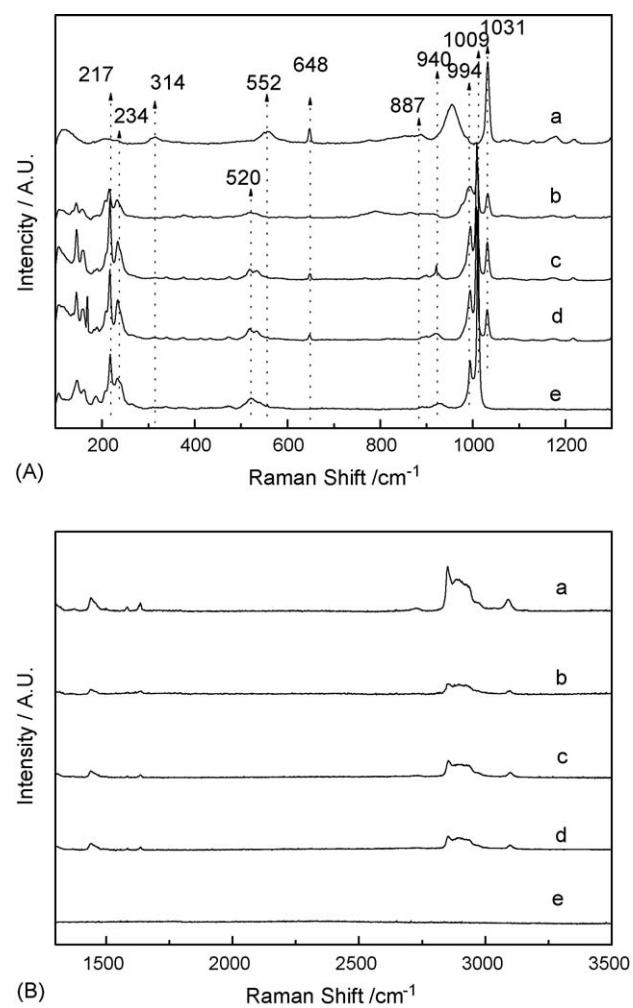

Fig. 3. Raman spectra of: (a) catalyst A1; (b) the recovered catalyst of A1 (Re-A1); (c) catalyst A2; (d) the recovered catalyst of A2 (Re-A2); (e) $H_3PW_{12}O_{40}{\cdot}H_2O$. The range of Raman shift of (A) is 100–1500 cm^{-1} and (B) is 1250–3500 cm^{-1}.

are corresponded to the ammonium cation. However, the Raman spectra of the recovered catalyst Re-A1 (see Fig. 3(A(b))) is very different from that of A1. The intensity of the 1031 cm^{-1} band decreases greatly, while the 648 cm^{-1} band almost disappears, indicating that the content of ammonium cation in the recovered catalyst is much lower after the reaction. In addition, the bands at 314, 887 and 964 cm^{-1} also disappear, indicating the absence of W–O_2H, free H_2O_2 and W=O.

There are some other difference between the recovered and the fresh A1 catalyst. First, the band at 552 cm^{-1} shifts to 520 cm^{-1}, such changes also occur in W(O_2) structure. Second, new bands at 217, 234, 994 and 1009 cm^{-1} appear, which are similar to those of spectra (c)—[π-$C_5H_5NC_{16}H_{33}]_3[PW_{12}O_{40}]$ (A2). It is also very interesting to find that the catalyst A2, Re-A2 and $H_3PW_{12}O_{40}$ show nearly the same Raman spectra besides the bands at 648 and 1031 cm^{-1} (see Fig. 3(A(c–e))), which show the same main bands at 217, 234, 520, 940, 994 and 1009 cm^{-1}. The very strong band at 1009 cm^{-1} is the characteristic of phosphatotungstate with Keggin structure, being attributed to $\upsilon_s(W = O_t)$ (O_t = terminal oxygen); the doublet strong bands at 940 and 994 cm^{-1} is assigned to $\upsilon_{as}(W = O_t)$; the band at 217 cm^{-1} can be attributed to $\upsilon_s(W\text{-}O_\mu)$ (O_μ = oxygen in bridge or μ-oxo) [33]. The presence of bridging oxygen indicates the presence of polymerization of W species (one W atom is linked to the other by bridging O). All the Raman spectra changes suggest that the recovered catalyst does not keep the initial structure of the fresh one, but polymerizes to a Keggin structure with bridging O_μ. In addition, there is almost no difference between spectra (c and d), both of which show the characteristic bands of phosphatotungstate with Keggin structure, suggesting that the Keggin structure is much more stable in the present system. Thus, the nearly same and lower TOF values of catalyst A2 and Re-A1 can be interpreted with their similar molecular structure.

In the 1250–3500 cm^{-1} range of Raman spectra, only bands of ammonium cation are observed because the Raman spectrum of $H_3PW_{12}O_{40}$ (see Fig. 3(B(e))) shows no bands in this region. Compared spectra (b) with (a), the intensity of all Raman bands are decreased, indicating the content of ammonium cation in the recovered catalyst is lowered. However, the intensity of the bands in spectra (b) is similar to that of (c) and (d), respectively, indicating that they have similar ammonium cation content. Spectrum (c) shows no obvious difference with (d), indicating the same molecular structure of the recovered Re-A2 as the fresh A2.

3.4. FT-IR spectra

In order to get further insight into the structure change of all the catalysts after reaction, FT-IR spectra were also collected, as shown in Fig. 4. For the purpose of easy assignment of IR bands, the FT-IR spectra of π-$C_5H_5NC_{16}H_{33}Cl$ (see Fig. 4(e)) was also measured and characteristic bands at 680, 715, 776, 1173 and 1209 cm^{-1} are observed. For the FT-IR spectra of the fresh A1 catalyst (Fig. 4(a)), main bands at 680, 715, 776, 886, 945, 1079, 1173 and 1209 cm^{-1} appear. Those at 680, 715, 776,

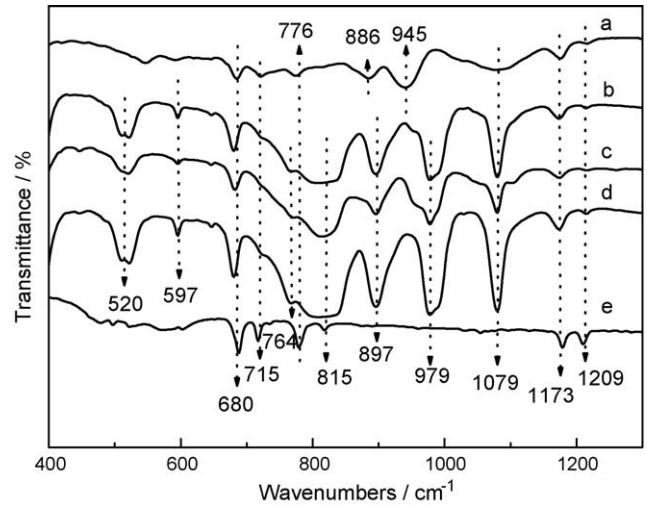

Fig. 4. FT-IR spectra of: (a) catalyst A1; (b) the recovered catalyst of A1 (Re-A1); (c) catalyst A2; (d) the recovered catalyst of A2 (Re-A2); (e) π-$C_5H_5NC_{16}H_{33}Cl$.

1173 and 1209 cm^{-1} are attributed to the ammonium cation according to the reference sample. The broad bands at 1079 and 945 cm^{-1} can be ascribed to the stretching mode of the P–O bond and the W=O bond, respectively [11]. Based on the results of the literatures [34–36], the IR band at 886 cm^{-1} can be attributed to the mode of $\upsilon(W\text{–}O_b\text{–}W)$ (corner-sharing). However, no band at 815 cm^{-1} (attributed to $\upsilon(W\text{–}O_c\text{–}W)$ (edge-sharing)) is observed, indicating the absence of polymerization of W species. In addition, no bands attributed to mode of υ(O–O) at 840 cm^{-1} is observed. However, there appears the band of υ(O–O) mode in the Raman spectra, suggesting that the symmetry of the local structure with O–O bond makes this band Raman active, but infrared inactive.

The FT-IR spectra of the recovered catalyst Re-A1 (see Fig. 4(b)) is totally different from that of A1, same as that in the Raman experiments. Interestingly, spectrum (b) is very similar to spectra (c and d), indicating the structure similarity of these three compounds. Besides of the bands at 680, 1173 and 1209 cm^{-1} that is due to the ammonium cation, characteristic bands at 1079, 979, 897, 815, 764, 597 and 520 cm^{-1} are also observed. The strong band at 1079 cm^{-1} is due to the stretching mode of the P–O bond [11,20–24]. Compared with spectrum (a), the shape of these bands changes greatly. The band at 945 cm^{-1} due to W=O [10,20–24] vibration in the fresh A1 catalyst shifts to 979 cm^{-1} in the recovered catalyst Re-A1. Similar result is also observed in the vibration region of $\upsilon(W\text{–}O_b\text{–}W)$, where the band shifts from 886 to 897 cm^{-1} [32–34]. The shifts indicate the changes of the bond lengths. In addition, a strong and broad band at 815 cm^{-1} appears, indicating the formation of a great number of $W\text{–}O_c\text{–}W$ bonds [34–36]. For the fresh catalyst, no band at 815 cm^{-1} is observed. Therefore, all WO_x species are in isolated state, and may be only linked to PO_4^{3-}. But for the recovered catalyst, WO_x species links not only to PO_4^{3-}, but also to other WO_x species according to the FT-IR results. The WO_x species polymerize by sharing the O atoms in corner. In conclude, the catalyst A1 polymerizes to $PW_{12}O_{40}^{3-}$ or other Keggin structure during the reaction,

which is in good agreement with that from Raman experiments. Similar result is also reported by Gao et al. [30]. Compared with spectra (c and d), no obvious difference can be observed, indicating that the catalyst A2 keeps its initial structure after the reaction, which suggests that the Keggin structure is much more stable in the present system. Same conclusion is also deduced from Raman spectroscopy as mentioned above, suggesting the reasonability of such conclusion in the present study.

3.5. ^{31}P NMR spectra

Liquid ^{31}P NMR spectra of the reaction system was also measured to investigate the structure change of the catalyst $[\pi\text{-}C_5H_5NC_{16}H_{33}]_3\{PO_4[WO_3]_4\}$ during the reaction, as shown in Fig. 5. The ^{31}P MAS NMR spectra of different solid catalysts are also shown in Fig. 6 for comparison. When H_2O_2 and cyclopentene are added to the mixture, the solid catalyst dissolves, and the ^{31}P NMR spectra changes greatly. As shown in Fig. 5, only peaks in the range of 2.0 to −1.0 ppm are observed. When the catalyst dissolves, three peaks are observed at 1.1, 0.7 and 0.26 ppm (see Fig. 5(a)), respectively. According to the results from literatures [21–24], it is reported that the ^{31}P NMR peaks at 4.1, 0.3 and −1.5 ppm are attributed to species from $[(PO_4)\{WO(O_2)_2\}_4]^{3-}$, $[(PO_4)\{WO(O_2)_2\}_2\{WO(O_2)_2(H_2O)\}]^{3-}$ and $[(PO_3(OH))\{WO(O_2)_2\}_2]^{2-}$, respectively. Thus, no $[(PO_4)\{WO(O_2)_2\}_4]^{3-}$ and $[(PO_3(OH))\ \{WO(O_2)_2\}_2]^{2-}$ are present, and only $[(PO_4)\{WO(O_2)_2\}_2\{WO(O_2)_2(H_2O)\}]^{3-}$ is possible to exist in the present reaction system. However, there appears more than one NMR peaks, suggesting that more than one P-containing species are present in the present system, which may be attributed to PO_4^{3-} species with one to three WO_x species being linked, or linked with other groups, such as H^+, H_2O, –OH, etc. Along with the reaction time, the peak at 1.1 ppm shifts to 1.0 ppm after being reacted for 1 h and finally to 0.8 ppm after the reaction was finished. Interestingly, the peak

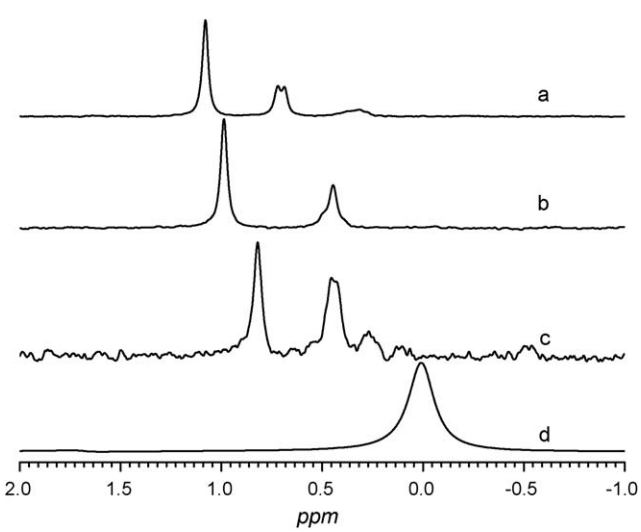

Fig. 5. ^{31}P NMR spectra of the catalyst A1 during reaction process. The reaction liquid was measured when: (a) the solid catalyst was dissolved and a pellucid liquid was obtained; (b) after 1 h reaction; (c) after 8 h reaction and only liquid is chosen to be measured; (d) H_3PO_4.

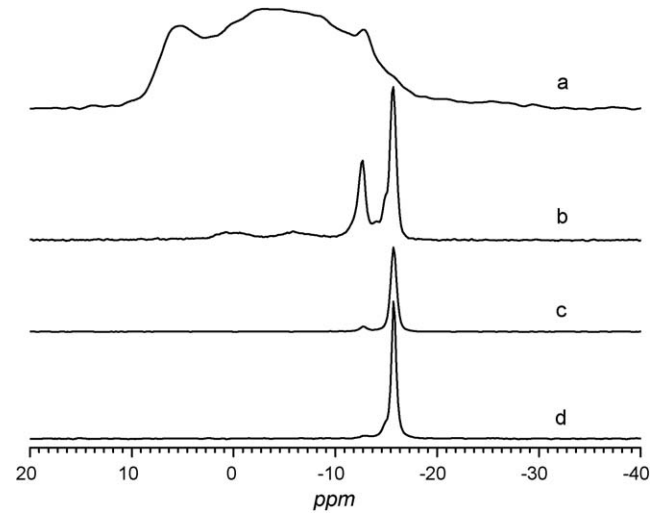

Fig. 6. ^{31}P MAS NMR spectra of catalyst: (a) fresh catalyst A1; (b) the recovered catalyst of A1 (Re-A1); (c) catalyst A2; (d) the recovered catalyst of A2 (Re-A2).

at 0.7 ppm in spectrum (a) also shows the same tendency. The phenomenon that these peaks all shift towards the lower field position of H_3PO_4 implies the degradation degree of the catalyst becomes much higher along with the reaction time. The treatment with strong aqueous H_2O_2 makes the insoluble catalyst to be degraded into smaller species, and become soluble in the reaction mixture. These soluble species are very active and can transfer oxygen to the C=C bond [30] and finally catalyze cyclopentene to glutaric acid. After the reaction, though most of the catalyst can precipitate itself because of the disappearance of H_2O_2, there is also some species that cannot precipitate and are soluble, being left in the resulting solution. Therefore, ^{31}P NMR peaks are also observed in the reaction liquid after reaction (Fig. 5(c)), which can be interpreted for the low recovery efficiency of the catalyst A1.

The structure of the recovered catalyst, which has been studied by Raman and FT-IR spectroscopy, is considered to change from that of the fresh one into the Keggin structure. However, what will happen in the ^{31}P MAS NMR spectroscopy is not clear yet. As shown in Fig. 6, the spectrum of the fresh A1 catalyst (Fig. 6(a)) shows a broad peak from 0 to −15.0 ppm, which can be assigned to heteropoly tungstophatosphates with the ratio of P/W from 1/2 to 1/12 [37]. Two additional shoulder peaks are also observed at 6.1 and −12.7 ppm, respectively. The one at 6.1 ppm might be due to species with higher P/W ratio [29]. The other one at −12.7 ppm is assigned to the $[PW_{11}O_{39}]^{7-}$ with Keggin structure [33,34]. Therefore, it is clear that catalyst A1 is not a pure compound as shown in the molecular formula with the P/W ratio of 1/4. Contrarily, it consists of several compounds with different P/W ratio, even small amounts of compounds with Keggin structure. However, Keggin structure has not been observed in Raman and FT-IR spectra because of its rather low content.

As also shown in Fig. 6, spectrum (b) of the recovered catalyst Re-A1 is totally different from that of the fresh one. Two main peaks at −12.6 and −15.7 ppm appeared, which are all characteristic peaks of compounds with Keggin structure

[35,36], and can be attributed to $(PW_{11}O_{39})^{7-}$ and $(PW_{12}O_{40})^{3-}$, respectively [29]. It is found that the WO_x and PO_4^{3-} species polymerize to form more stable Keggin structure after the reaction, resulting in the precipitate of $[\pi\text{-}C_5H_5NC_{16}H_{33}]_7[PW_{11}O_{39}]$ and $[\pi\text{-}C_5H_5NC_{16}H_{33}]_3\,[PW_{12}O_{40}]$ from the reaction mixture. Then the catalyst can be recovered and reused easily. $[\pi\text{-}C_5H_5NC_{16}H_{33}]_7[PW_{11}O_{39}]$ is also synthesized independently following the procedure reported previously [38] and the mixture of compound $[\pi\text{-}C_5H_5NC_{16}H_{33}]_7[PW_{11}O_{39}]$ and $[\pi\text{-}C_5H_5NC_{16}H_{33}]_3\,[PW_{12}O_{40}]$ is used as catalyst in this reaction, for the purpose to simulate the recovered catalyst Re-A1. 89.6% GAC yield was obtained, little higher than the individual $[\pi\text{-}C_5H_5NC_{16}H_{33}]_3\,[PW_{12}O_{40}]$ catalyst (85.6%), but it is still much lower than that obtained on the recovered catalyst Re-A1, suggesting that the recovered catalyst Re-A1 is not a simple mixture of A1 and A2, however, the reason is not clear now. In addition, there appear two small and broad peaks located from 5 to −10 ppm, suggesting that other species are also formed after the reaction, however, the amount is very small and it is not discussed in the present study.

The ^{31}P MAS NMR spectra of the catalyst $[\pi\text{-}C_5H_5NC_{16}H_{33}]_3[PW_{12}O_{40}]$ (A2) and the recovered one (Re-A2) are also recorded, as shown in Fig. 6(c and d), respectively, both of which are nearly the same, and shows a single peak at −15.7 ppm. The results indicate that the catalysts with Keggin structure can keep its initial structure and precipitate easily from the reaction system after the reaction. A small peak at −12.6 ppm is also observed in spectrum (c), suggesting that a small amounts of $[\pi\text{-}C_5H_5NC_{16}H_{33}]_7[PW_{11}O_{39}]$ was produced during the preparation of $[\pi\text{-}C_5H_5NC_{16}H_{33}]_3[PW_{12}O_{40}]$. However, in spectrum (d), the peak at this position is much smaller and even cannot be easily distinguished, thus, the $(PW_{12}O_{40})^{3-}$ structure may be more stable than $(PW_{11}O_{39})^{7-}$ in the present system and much easier to be formed. This result is also in good agreement with those from Raman and FT-IR.

4. Conclusions

Good glutaric acid yield of 83.1% was obtained in the selective oxidation of cyclopentene with aqueous H_2O_2 over a reaction-controlled phase-transfer catalyst $[\pi\text{-}C_5H_5NC_{16}H_{33}]_3\{PO_4[WO_3]_4\}$(A1), which is much more active than the homogeneous tungstic acid catalyst. The fresh A1 catalyst is insoluble in the reaction system at first but become soluble when mixed with strong hydrogen peroxide and precipitates again after the reaction, resulting in the easy separation and convenient recovery of the catalyst. In addition, the yield of GAC is even much higher over the recovered catalyst, although the activity is lowered than that of the fresh one. All the catalysts before and after reaction were characterized with TG, Raman, FT-IR and ^{31}P NMR spectroscopy. It is found that the fresh catalyst is a complex mixture and can be degraded into small active species during the reaction. After the reaction, the W content increases and the ammonium cation content decreases for the recovered catalyst. The WO_x species polymerize by forming W–O_c–W bond and form more stable Keggin structure as $[\pi\text{-}C_5H_5NC_{16}H_{33}]_7[PW_{11}O_{39}]$ and $[\pi\text{-}C_5H_5NC_{16}H_{33}]_3\,[PW_{12}O_{40}]$. Studies on the detailed structure of the degraded species are being under way.

Acknowledgments

This work was financially supported by the Major State Basic Resource Development Program (Grant No. 2003CB615807), NSFC (Project 20407006, 20573024) and the Natural Science Foundation of Shanghai Science & Technology Committee (02DJ14021).

References

[1] M. Besson, F. Gauthard, B. Horvath, P. Gallezot, J. Phys. Chem. B 109 (2005) 2461.
[2] R.W. Johnson, C.M. Pollock, R.R. Cantrell, in: M. Bickford, J.I. Kroschwitz (Eds.),3rd ed., Kirk-Othmer Encyclopedia of Chemical Technology, vol. 8, John Wiley & Sons, New York, 1993.
[3] A.K. Sureh, M.M. Sharma, T. Sridhar, Ind. Eng. Chem. Res. 39 (2000) 3958.
[4] A. Castellan, J.C.J. Bart, S. Cavallarro, Catal. Today 9 (1991), 237, 255, 284.
[5] K. Sato, M. Aoki, R. Noyori, Science 281 (1998) 1646.
[6] R. Noyori, M. Aoki, K. Sato, Chem. Commun. (2003) 1977.
[7] H. Chen, W. Dai, X. Yang, R. Gao, Y. Cao, K. Fan, Petrochem. Technol. 35 (2) (2006) 118 (in Chinese).
[8] C. Venturello, E. Alneri, M. Ricci, J. Org. Chem 48 (1983) 3831.
[9] C. Venturello, R. D'Alosio, J.C. Bart, M. Riai, J. Mol. Catal. 32 (1985) 107.
[10] C. Venturello, M. Ricci, J. Org. Chem. 51 (1986) 1599.
[11] C. Venturello, R. D'Aloisio, J. Org. Chem. 53 (1988) 1553.
[12] P. Fantucci, S. Lolli, C. Venturello, J. Catal. 169 (1997) 228.
[13] Y. Ishii, K. Yamawaki, T. Yoshida, T. Ura, H. Yamada, M. Ogawe, J. Org. Chem. 52 (1987) 1868.
[14] Y. Ishii, K. Yamawaki, T. Ura, H. Yamada, T. Yoshida, M. Ogawe, J. Org. Chem. 53 (1988) 3587.
[15] S. Sakaue, Y. Sakata, Y. Nishiyama, Y. Ishii, Chem. Lett. 2 (1992) 289.
[16] S. Sakaue, T. Tsubakino, Y. Nishiyama, Y. Ishii, J. Org. Chem. 58 (1993) 3633.
[17] Y. Ishii, H. Tanaka, Y. Nishiyama, Chem. Lett. 1 (1994) 1.
[18] K. Nakayama, M. Hamamoto, Y. Nishiyama, Y. Ishii, Chem. Lett. 10 (1993) 1699.
[19] M. Hamamoto, K. Nakayama, Y. Nishiyama, Y. Ishii, J. Org. Chem. 58 (1993) 6421.
[20] C. Aubry, G. Chottard, N. Platzer, J.M. Brégeault, R. Thouvenot, F. Chaureau, C. Huet, H. Ledon, Inorg. Chem. 30 (1991) 4409.
[21] L. Sales, C. Aubry, R. Thouvenot, F. Robert, C.D. Morin, G. Chottard, H. Ledon, Y. Jeannin, J.M. Brégeault, Inorg. Chem. 33 (1994) 871.
[22] D.C. Duncan, R.C. Chambers, E. Hecht, C.L. Hill, J. Am. Chem. Soc. 117 (1995) 681.
[23] L. Salles, J.Y. Piquemal, R. Thouvenot, C. Minot, J.M. Brégeault, J. Mol. Catal. A 117 (1997) 375.
[24] N.M. Grecley, W.P. Griffith, A.C. Laemmel, H.S. Nogueira, B.C. Parkin, J. Mol. Catal. A 117 (1997) 185.
[25] H. Zeng, G.R. Newkome, C.L. Hill, Angew. Chem. Int. Ed. 39 (2000) 1771.
[26] L. Plault, A. Hauseler, S. Nlate, D. Astruc, J. Ruiz, S. Catard, R. Neumann, Angew. Chem. Int. Ed. 43 (2004) 2924.
[27] S. Nalte, D. Astruc, R. Neumann, Adv. Synth. Catal. 346 (2004) 1445.
[28] Z. Xi, N. Zhou, Y. Sun, K. Li, Science 292 (2001) 1139.
[29] Y. Chen, J. Zhang, X. Liu, J. Gao, X. Han, X. Bao, N. Zhou, S. Gao, Z. Xi, Catal. Lett. 93 (2004) 41.
[30] J. Gao, Y. Chen, B. Han, Z. Feng, C. Li, N. Zhou, S. Gao, Z. Xi, J. Mol. Catal. A 210 (2004) 197.
[31] Y. Sun, Z. Xi, G. Gao, J. Mol. Catal. A 166 (2001) 219.
[32] N.J. Campbell, A.C. Dengel, C.J. Edwards, W.P. Griffith, J. Chem. Soc., Dalton Trans. (1989) 1203.

[33] C. R'Deltcheff, M. Fournier, R. Franck, R. Thouvenot, Inorg. Chem. 22 (1983) 207.
[34] E. Radkov, R.H. Beer, Polyhedron 14 (1995) 2139.
[35] N.I. Kuznetsova, L.G. Detusheva, L.I. Kuznetsova, M.A. Fedotov, V.A. Likholobov, J. Mol. Catal. A 114 (1996) 131.
[36] L.R. Pizzio, C.V. Cáceres, M.N. Blanco, Appl. Surf. Sci. 151 (1999) 91.
[37] M.T. Pope, Heteropoly and Isopoly Oxometalates, Springer-Verlag, Berlin, 1983, p. 66.
[38] C. Brevard, R. Schimpf, G. Tourne, C.M. Tournet, J. Am. Chem. Soc. 105 (1983) 7060.